Theoretical investigations on the mechanism of chalcogens exchange reaction between P(V) and P(III) compounds

Martin Kullberg [a], Jacek Stawinski [a,b,*]

[a] *Department of Organic Chemistry, Arrhenius Laboratory, Stockholm University, S-106 91 Stockholm, Sweden*
[b] *Institute of Bioorganic Chemistry, Polish Academy of Sciences, Noskowskiego 12/14, 61-704 Poznan, Poland*

Abstract

Two mechanistic pathways for chalcogens transfer from P(V) to P(III) compounds were explored using density functional theory calculations and for both of them the corresponding transition states were identified. The calculations showed that transfer of sulfur and selenium proceeds most likely via an X-philic attack of the phosphorus nucleophile on the chalcogen, while for the oxygen transfer reaction, a mechanism involving a three-membered cyclic transition state is equally likely.
© 2004 Elsevier B.V. All rights reserved.

Keywords: Chalcogens; Exchange; Calculations

1. Introduction

The transfer of chalcogens from P(V) to P(III) compounds was first discovered by Gottlieb in 1932 [1] and since then it has been used for the preparations of various P(V) derivatives containing either sulfur [1] or selenium [2–4]. Alternatively, this reaction can be used to reduce P(V) compounds into the corresponding P(III) derivatives [3–10]. Although the transformations involving transfer of sulfur or selenium are rather common, there are only a few reports in literature on the oxygen transfer reaction [11,12] and these involve exclusively phosphine oxides with at least one leaving group as donors.

One can envisage two likely mechanisms for the chalcogens transfer reactions (Scheme 1). Mechanism 1, which involves a nucleophilic attack of a P(III) species on the phosphorus centre of a P(V) compound that may proceed via a three-membered cyclic transition state, and Mechanism 2, which is an X-philic attack of a P(III) compound on the chalcogen of the P(V) species and involves a linear transition state. The former mechanism, postulated for the selenium exchange reaction [2], could account for the fact that oxygen transfer is facilitated by the presence of strong electron-withdrawing groups [11,12], while the later one, was claimed to be consistent with the observed a second order kinetics for the sulfur transfer process [8] and it was also proposed for the oxygen transfer from phosphorus oxychloride to trialkylphosphine [13].

To gain further insight into the chalcogen transfer process and to determine through which mechanism these reactions proceed, we undertook a theoretical study using density functional theory calculation on the model reactions showed in Scheme 2. We also hoped that the knowledge gained will be helpful in a rational design of new, effective chalcogen transferring and reducing reagents for phosphorus compounds.

---

* Corresponding author. Tel.: +46 8 16 24 85; fax: +46 8 15 49 08.
E-mail address: js@organ.su.se (J. Stawinski).

Mechanism 1:

Mechanism 2:
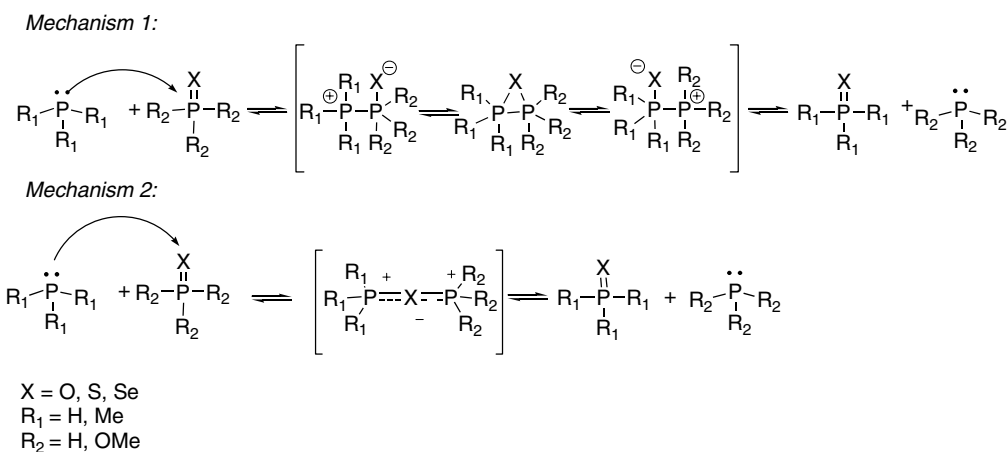
X = O, S, Se
R_1 = H, Me
R_2 = H, OMe
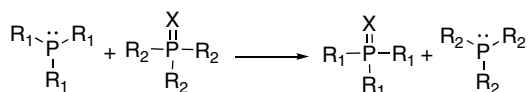
Scheme 1.

X = O, S, Se; R_1 = H, Me; R_2 = H, OMe

Scheme 2.

2. Computational methods

All DFT calculations were performed with GAUSSIAN98 package [14] using the B3LYP [15–17] method of density functional theory at the 6-31G* level of theory. All transition states were found by relaxed potential energy surface scanning along the reaction coordinate and then optimized by TS optimization. All stationary points were characterized as minima or transition states by analytical frequency calculations. Visualization of the orbitals was carried out with GaussView 3.0.

3. Results and discussion

3.1. Geometries of the starting materials

Our optimized geometries of the starting materials show reasonable to good agreement with the experimentally determined structures reported in the literature [18]. Selected structural data and energies are collected in Table 1. Whenever experimentally determined data were available, these values have been included for comparison.

It was found that in vacuum some reactants gain stabilisation by forming contact complexes, probably through electrostatic interactions of the dipoles of the molecules. To make a meaningful comparisons between the reactions investigated, the contact complexes of all the reactants and the products were calculated and used as starting structures for the reactions. The energy data for these complexes are summarised in Table 2.

To get some insight into possible interactions between P(V) and P(III) substrates during chalcogens

Table 1
Geometries[a,b] and energy of starting materials

Molecule	Energy, H	0-point E, kcal/mol	P = X, Å	P–Y, Å	Z–Y, Å	$\angle XPY$, °	$\angle YPY$, °	$\angle PYZ$, °
H_3P	−343.1403	15.2024		1.424 (1.412)			93.37 (93.36)	
H_3PO	−418.3577	19.5875	1.494	1.420		117.61	100.17	
H_3PS	−741.3326	18.2595	1.9603	1.4184		118.10	99.62	
H_3PSe	−2742.5239	17.8801	2.0999	1.4178		118.30	99.37	
Me_3P	−461.0984	71.1797		1.8673 (1.847)			99.35 (98.6)	
Me_3PO	−536.3530	74.1125	1.5013 (1.489)	1.8350 (1.771)		114.24 (113.1)	104.31 (105.9)	
Me_3PS	−859.3223	73.0894	1.97182 (1.959)	1.8405 (1.798)		114.56 (113.2)	103.94 (105.8)	
Me_3PSe	−2860.5123	72.6015	2.1103 (2111)	1.8421 (1.786)		114.85 (113.1)	103.60 (105.7)	
MeO_3P	−686.7641	80.6503		1.6540	1.4264		105.18	132.88
MeO_3PO	−762.0471	84.8259	1.4789	1.6076	1.4412	115.38	103.01	119.99
MeO_3PS	−1085.0046	83.4280	1.9334	1.6160	1.4401	116.21	102.01	120.69
MeO_3PSe	−3086.1646	81.9194	2.0578	1.6228	1.4305	111.42	107.46	131.97

[a] Mean values are quoted.
[b] Measured structure from litterature is given within () when availible.

Table 2
Energies of contact complexes

Contact complex	Energy, H	0-point E, kcal/mol
H_3PO H_3P	−761.5005	35.2935
H_3PS H_3P	−1084.4728	33.5494
H_3PSe H_3P	−3085.6654	33.2494
Me_3PO MeO_3P	−1223.1313	155.6822
Me_3PS MeO_3P	−1546.0977	154.3262
Me_3PSe MeO_3P	−3547.2991	154.5506
MeO_3PO Me_3P	−1223.1519	156.6844
MeO_3PS Me_3P	−1546.1078	155.1035
MeO_3PSe Me_3P	−3547.3038	155.2194

exchange process, first we investigated geometry of the frontier molecular orbitals of our model systems. Since Mechanism 1 and Mechanism 2 (see Scheme 1) involve an attack of a phosphorus nucleophile, geometry of HOMO of a P(III) species and LUMO of the corresponding chalcogenides (Fig. 1), may provide a qualitative way to determine if the proposed mechanisms are reasonable.

Inspection of Fig. 1 shows that LUMO for phosphine sulfide and phosphine selenide are similar in shape and feature strong lobes pointing straight out from the chalcogen, that may invite a nucleophilic attack on this centre. The other part of the orbitals centred on the phosphorus seems to be buried inside the occupied orbitals, and thus may be less accessible for nucleophilic attack.

LUMO for phosphine oxide differs significantly from those of the corresponding sulfide and selenide. This LUMO is more diffuse and has different geometry than LUMO of the other chalcogens. Interestingly enough, for phosphine oxide LUMO + 1 has the appearance that is very close to those of the LUMO of the sulfide and the selenide, although, this orbital is more centred on the phosphorus. Taking these into account, one may expect that for phosphine oxide, both phosphorus (Mechanism 1) and oxygen centre (Mechanism 2) may be available for attack of the phosphorus nucleophile.

3.2. Transition states of chalcogens transfer

The transition state structures for the investigated reactions were localised by incremental scanning of the potential energy surface along the reaction coordinates. For the X-philic attack (Mechanism 2) this was done by varying the distance between the attacking phosphorus nucleophile and the corresponding chalcogen, and in the instance of Mechanism 1, by varying the distance between the phosphorus nucleophile and the phosphorus centre in chalcogenides. This strategy worked well for Mechanism 2 (the attack at the chalcogen), for which we could pinpoint roughly the whereabouts of the transition state and perform optimisation to the TS.

In the case of Mechanism 1, this protocol was more troublesome and the curvature could not be mapped well enough to get a rough idea of the transition states whereabouts. For this reason exhausting frequency calculations were performed along the reaction coordinates and when negative frequencies corresponding to movement along the reaction coordinate were found, these structures were used as starting point for the TS optimisation.

The transition state structures of X-philic attack on the chalcogens (Mechanism 2) show a striking difference between the transfer of sulfur and selenium, on one hand, and the transfer of oxygen reaction, on the other one (Fig. 2). For the reactions involving transfer of sulfur and selenium the corresponding transition states are almost completely linear, while that for the oxygen transfer, it is bent and resembles more the transition states for Mechanism 2 (vide infra and Fig. 3). All the localised transition states structures were identified as true TS by analytical frequency calculations that revealed only one negative frequency corresponding to the movements along the reaction coordinates. The energy and the selected geometrical data of these transition states are summarized in Table 3.
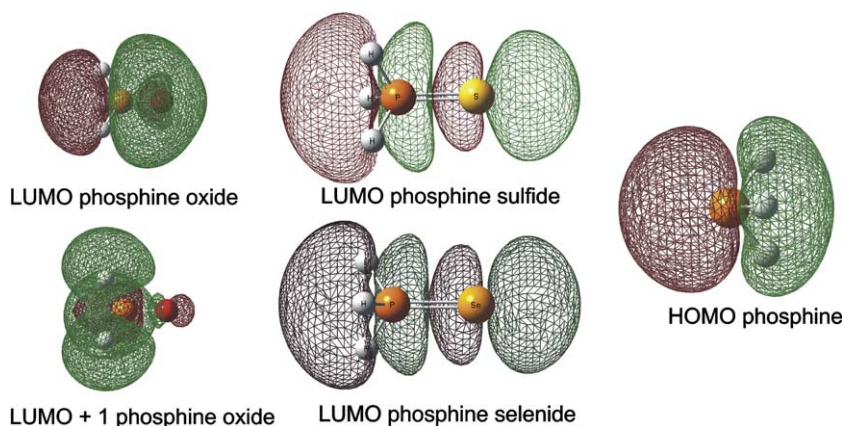

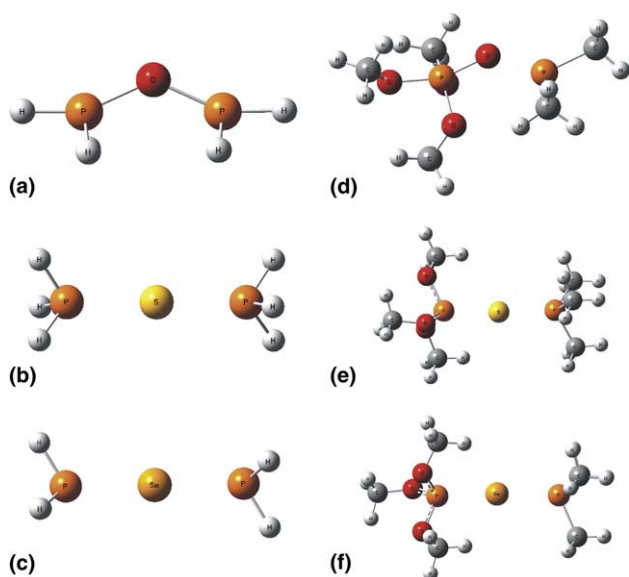Fig. 1. Frontier molecular orbitals for phosphine chalcogenides and phosphine.

Fig. 2. Localized TS of the chalcogens exchange reactions for Mechanism 2. (a) $H_3PO + H_3P$; (b) $H_3PS + H_3P$; (c) $H_3PSe + H_3P$; (d) $(MeO)_3PO + Me_3P$; (e) $(MeO)_3PS + Me_3P$; (f) $(MeO)_3PSe + Me_3P$.

Fig. 3 shows examples of transition state structures for chalcogen transfer reactions proceeding through Mechanism 1. For the reactions between $H_3P=Ch + H_3P$, no transition states could be localised along the reaction coordinates involving the initial nucleophilic attack at phosphorus centre. Instead, only three-membered cyclic TS corresponding to the edge attack of the phosphorus nucleophile on the $P=Ch$ bond were found, which indicate that in vacuum these are essentially cycloaddition reactions.

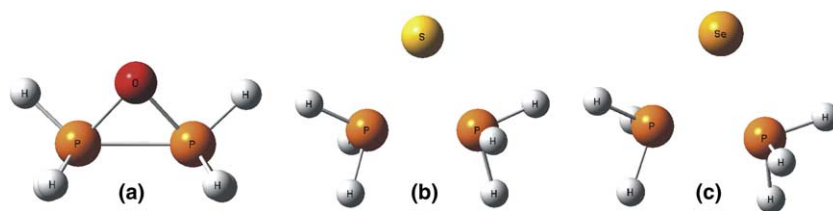The transition states localised were characterised by frequency calculations and their geometry and energy data are summarized in Table 4.

3.3. Activation energies of the reaction

In the energy diagrams, energies of all contact complexes were set to 0 regardless of their initial values to facilitate comparison of the activation energies of different reactions. All energies were compensated for the zero point vibrational energy.

Fig. 4 shows the energy diagrams for the edge attack of phosphorus nucleophile on the $P=Ch$ bond (Mechanism 1). From this data, it is apparent that activation energies for all investigated reactions are very high (above 50 kcal/mol) and contrary to the experimental data, the energy barriers are similar for all of the chalcogens. This alone is a strong indication that Mechanism 1 cannot be a general mechanism for chalcogens transfer reactions.
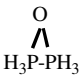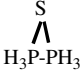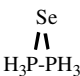
In contrast to these, activation energies for the X-philic attack (Mechanism 2) showed the expected trend for the investigated chalcogenides (Fig. 5). Thus, the reactions involving transfer of oxygen had very high activation energy (ca. 56–69 kcal/mol), while those for sulfur and selenium transfer, were significantly less energy demanding (for sulfur, ca. 7–20 kcal/mol, and for selenium, ca. 4–10 kcal/mol). This trend is in agreement with the observed reactivity of phosphine chalcogenides in the chalcogen exchange reactions between P(V) and P(III) compounds. The activation energy for the sulfur transfer reaction was of the same order of magnitude as the activation energy for the reaction of triphenyl-

Fig. 3. Localized TS of the chalcogens exchange reactions for Mechanism 1. (a) $H_3PO + H_3P$; (b) $H_3PS + H_3P$; (c) $H_3PSe + H_3P$.

Table 3
Geometries[a] and energy of transition states for Mechanism 2

Transition state	Energy, H	0-point E, kcal/mol	P^1–X, Å	P^2–X, Å	P^1–Y, Å	P^2–Y, Å	∠PXP, °	Negative frequency
H_3P–O–PH_3	−761.4129	34.2360	1.8057				130.71	−724.96
H_3P–S–PH_3	−1084.4421	33.1964	2.3704				179.95	−351.23
H_3P–Se–PH_3	−3085.6505	33.22939	2.4734				180	−201.45
MeO_3P^1–O–P^2Me_3	−1223.0451	154.3283	1.7196	1.9298	1.6803	1.8521	134.93	−625.55
MeO_3P^1–S–P^2Me_3	−1546.0640	154.3262	2.3524	2.4027	1.6422	1.8513	177.14	−334.02
MeO_3P^1–Se–P^2Me_3	−3547.2781	154.0133	2.4376	2.5155	1.6398	1.8518	173.72	−174.74

[a] Mean values are quoted.

Table 4
Geometries[a] and energy of transition states for Mechanism 1

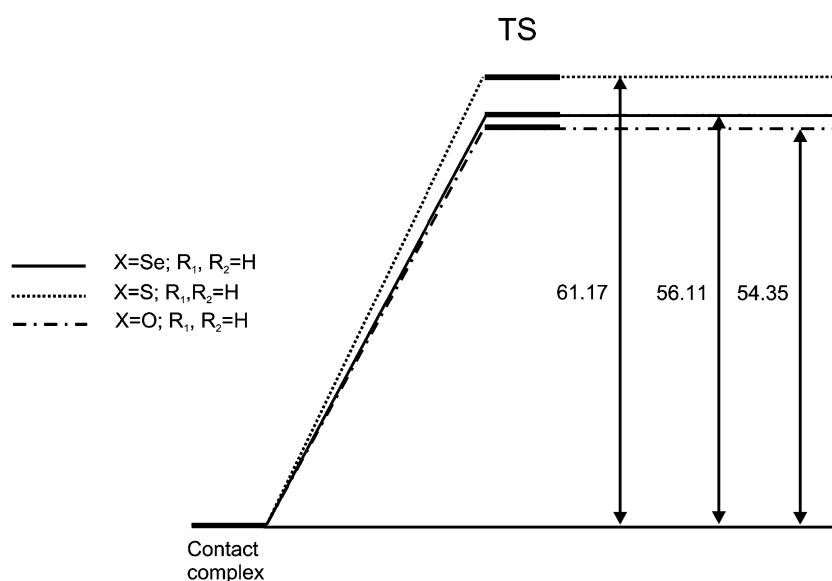| Transition state	Energy, H	0-point E, kcal/mol	P^1–X, Å	P–P, Å	∠PXP, °	Negative Frequency
O ∧ H_3P-PH_3	−761.4119	36.5292	1.7402	2.2343	79.88	−486.59
S ∧ H_3P-PH_3	−1084.3732	34.8956	2.2922	2.3402	61.39	−557.62
Se ∧ H_3P-PH_3	−3085.5743	34.2927	2.4318	2.3799	58.59	−538.87

[a] Mean values are quoted.

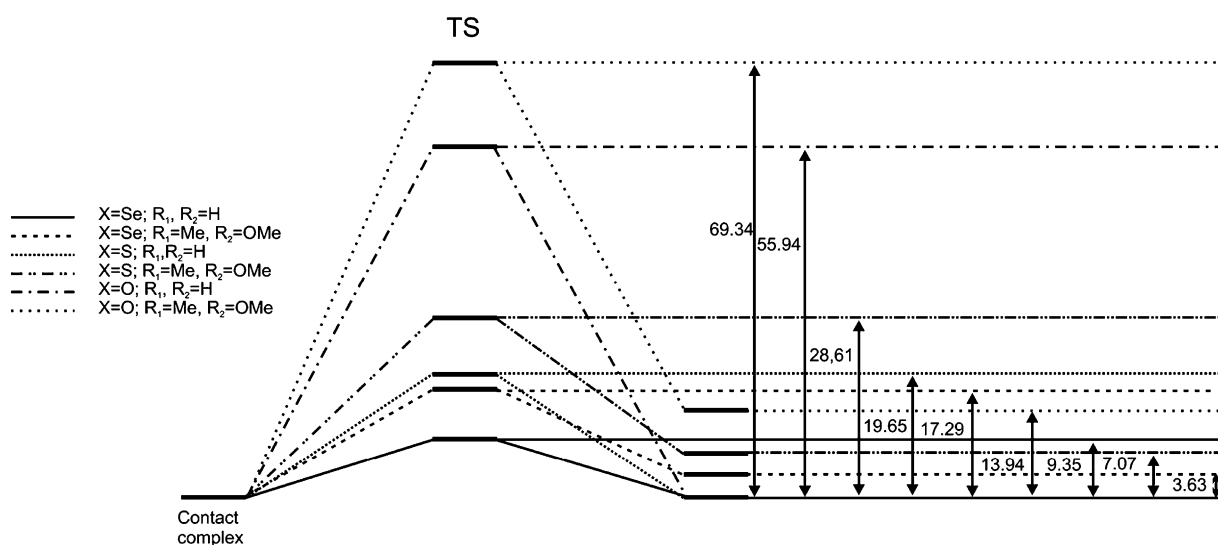Fig. 4. Activation energies (in kcal/mol) of the reactions $R_3^2X + R_3^1P$ for Mechanism 1.

Fig. 5. Activation energies (in kcal/mol) for the reactions $R_3^2X + R_3^1P$ for Mechanism 2.

phosphine sulfide and tributylphosphine reported in literature [8] (~22.3 kcal/mol).

It is worth noting, however, that for the oxygen transfer, activation energies of the reaction $H_3P{=}O + H_3P$ for Mechanism 1 and Mechanism 2 are both similar (ca. 54.4 and 55.9 kcal/mol, respectively), and favour only slightly the exchange process via Mechanism 1.

4. Conclusions

From the nine transition states localised and characterized, we got the activation energies for two alternative mechanisms for the chalcogens transfer reactions from P(V) to P(III) compounds. The results strongly suggest that transfer of sulfur and selenium proceeds most likely via a direct attack of the phosphorus nucleophile at the chalcogen centre and involves a linear transition state. By this mechanism, the transfer of sulfur and selenium can safely be assumed to proceed stereospecifically with retention of configuration at phosphorus centres.

For the oxygen transfer reaction, however, the results are somewhat inconclusive since attack of a phosphorus nucleophile on the chalcogen and on the phosphorus centre of a P(V) component have similar activation energies. This energetic barrier is very high and effectively prevents reduction of P(V) phosphoryl compounds or oxidation of P(III) derivatives by phosphoryl compounds, except for special cases.

References

[1] H.B. Gottlieb, J. Am. Chem. Soc. 54 (1932) 748–751.
[2] M. Kullberg, M. Bollmark, J. Stawinski, Collect. Symp. Ser. 5 (2002) 290–294.
[3] M. Bollmark, J. Stawinski, Chem. Commun. 8 (2001) 771–772.
[4] M. Bollmark, M. Kullberg, J. Stawinski, Tetrahedron Lett. 43 (2002) 515–518.
[5] D.L. Field, P.M. Wilkinson, Tetrahedron Lett. 38 (1997) 2779–2782.
[6] P.C. Crofts, D.M. Parker, J. Chem. Soc. C (1970) 332–336.
[7] L. Maier, Helv. Chim. Acta 54 (1971) 1651–1660.
[8] K.D. Berlin, G.H. Hopper, Proc. Okla. Acad. Sci. 46 (1966) 85–95.
[9] S. Trofimenko, A.L. Rheingold, C.D. Incarvito, Ang. Chem. Int. Ed. Eng. 42 (2003) 3506–3509.
[10] D.H. Brown, R.J. Cross, R. Keat, J. Chem. Soc. Dalton (1980) 871–874.
[11] L.F. Grantham, Diss. Abst. 19 (1959) 898.
[12] N. Zhang, J.E. Casida, J. Org. Chem. 66 (2001) 327–329.
[13] A.M. Aquiar, Diss. Abst. 21 (1960) 457.
[14] Gaussian 98 (Revision A.3).
[15] A.D. Becke, J. Chem. Phys. 98 (1993) 5648–5652.
[16] J.A. Pople, M. Head-Gordon, D.J. Fox, K. Raghavachari, L.A. Curtiss, J. Chem. Phys. 90 (1989) 5622.
[17] L.A. Curtiss, C. Jones, G.W. Trucks, K. Raghavachari, J.A. Pople, J. Chem. Phys. 93 (1990) 2537.
[18] G.D. Gilheany, Chem. Rev. 94 (1994) 1339–1374.